Complex domain-wall dynamics in compressively strained Ga$_{1-x}$Mn$_x$As epilayers

Liza Herrera Diez,[1] Reinhard K. Kremer,[1] Axel Enders,[1,*] Matthias Rössle,[1,†] Erhan Arac,[1,‡] Jan Honolka,[1,§] Klaus Kern,[1]
Ernesto Placidi,[2] and Fabrizio Arciprete[2]

[1]*Max-Planck-Institut für Festkörperforschung, Heisenbergstrasse 1, 70569 Stuttgart, Germany*
[2]*Dipartimento di Fisica, Università di Roma "Tor Vergata," CNR-INFM, Via della Ricerca Scientifica 1, I-00133 Roma, Italy*

The domain-wall-induced reversal dynamics in compressively strained Ga$_{1-x}$Mn$_x$As was studied employing the magneto-optical Kerr effect and Kerr microscopy. Due to the influence of a uniaxial part in the in-plane magnetic anisotropy $90° \pm \delta$ domain walls with considerably different dynamic behavior are observed. While the $90° + \delta$ reversal is identified to be propagation dominated with a small number of domains, the case of $90° - \delta$ reversal involves a larger number of nucleation centers. The domain-wall nucleation/propagation energies ϵ for both transitions are estimated using model calculations from which we conclude that single domain devices can be achievable using the $90° + \delta$ mode.

The discovery of the ferromagnetic semiconductor Ga$_{1-x}$Mn$_x$As and the possible implementation into spintronic devices triggered great interest in understanding its fundamental properties.[1] The linkage between carrier density and magnetic properties in this hole-mediated ferromagnet allows tuning of its magnetic properties such as the Curie temperature (T_c) upon changing the carrier concentration.[2,3] In addition, magnetic domain-wall (DW) logic operations may be implemented[4] including magnetoresistive read-outs. However, any application in this direction requires full control over magnetic reversal dynamics, which in most cases happens via the nucleation and propagation of domain walls.

A good understanding of the magnetic anisotropy landscape is also required not only for the design of magnetoresistive devices but also because magnetic anisotropy can manifest in the domain-wall dynamics. The magnitude of the magnetic anisotropy is related to important parameters such as the domain-wall energy and width,[5] which can determine a process to be propagation or nucleation dominated. This can be very well visualized in the effect of a nonuniform anisotropy distribution in simulated reverse domain patterns.[6]

So far, domain-wall studies by means of Kerr microscopy (KM) in Ga$_{1-x}$Mn$_x$As have been mostly performed in films with tensile strain where the magnetization pointed perpendicular to the plane.[7] Ga$_{1-x}$Mn$_x$As with in-plane magnetization has been extensively studied using magnetotransport measurements.[8,9] However, this technique does not provide spatially resolved information about DW nucleation and propagation processes. In this study we present the direct observation of DW motion in compressively strained Ga$_{1-x}$Mn$_x$As by KM and the dependence of the DW dynamics on the direction of the applied magnetic field. While an earlier magneto-optical study in the literature[10] did not address possible anisotropies in the DW dynamics, our KM results reveal a distinct anisotropy in the DW dynamics dependent on the direction of the applied magnetic field with respect to the crystal axes. From the analysis of angle-resolved magneto-optical Kerr effect (MOKE) measurements, we attribute this anisotropy to the existence of two different types of DWs. All measurements were done on Hall

bar devices of 150 μm width, patterned in $[1\bar{1}0]$ and $[110]$ directions using photolithography.

The Ga$_{1-x}$Mn$_x$As sample was grown in a RIBER 32 molecular beam epitaxy (MBE) system equipped with a reflection high-energy electron diffraction (RHEED) setup for *in situ* monitoring of the growth. Prior to Ga$_{1-x}$Mn$_x$As deposition, a GaAs buffer layer of approximately 400 nm was grown on a Si-doped GaAs(001) substrate ($n \approx 10^{18}$ cm^{-3}), in As$_4$ overflow at $\approx$590 °C, and at a rate of 0.8 μm/h. After 10 min post-growth annealing under As$_4$ flux, the temperature was lowered to 270 °C for Ga$_{1-x}$Mn$_x$As deposition. Using an As$_4$:Ga flux ratio of 50 a 170 nm Ga$_{1-x}$Mn$_x$As layer was grown at a rate of 0.33 ML/s. During Ga$_{1-x}$Mn$_x$As growth a clear two-dimensional (2D) (1×2) RHEED pattern was observed with no indication of MnAs precipitates at the surface (no spotty RHEED pattern). Ga, Mn, and As$_4$ fluxes were calibrated by an ion gauge placed in the substrate position [beam equivalent pressure (BEP)]. A nominal Mn concentration of $x = (2.3 \pm 0.1)\%$ was estimated on the basis of flux (BEP) ratios of As$_4$, Ga, and Mn. The high quality of the grown films has also been verified by measuring the x-ray diffraction pattern of the film. Typical diffraction profiles for Ga$_{1-x}$Mn$_x$As/GaAs structures have been found, which contain two distinct peaks around the (004) Bragg reflex corresponding to the GaAs and Ga$_{1-x}$Mn$_x$As layers.[11]

Longitudinal MOKE measurements have been done at a temperature of $T \sim 3$ K, changing the direction of the in-plane applied field with respect to the crystal axes in order to map the coercivities and thus the magnetic anisotropy. Along the $[110]$ and $[1\bar{1}0]$ directions we observe only one switching field within the available field range, while in other directions as in the case of the $[100]$ direction [Fig. 1(a)], two transitions and an intermediate plateau were found. The observed dependences of the switching fields on the direction of the applied field are consistent with the results already found by other authors[9] in Ga$_{1-x}$Mn$_x$As with similar Mn concentration. In addition, the magnetization value as a function of temperature presented in Fig. 1(b) was measured using a superconducting quantum interference device (SQUID) magnetometer. The Curie temperature and saturation magnetization values determined from this measurement are T_C
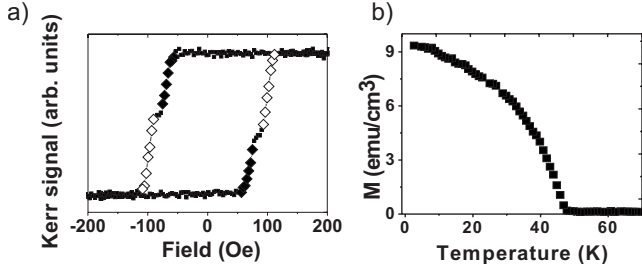
FIG. 1. (a) Two-step hysteresis loop measured with the field applied along [100] at T=3 K. The first- and second-switching events are indicated by filled and open symbols, respectively. (b) Magnetization as a function of temperature measured at H=1 T with SQUID in zero-field cooling.

=(48 ± 2) K and M=(9.4 ± 0.1) emu/cm^3, respectively.

Prior to every single KM measurement the sample was saturated at a magnetic field of 1000 Oe. The transition was then triggered by applying a constant field of opposite polarity corresponding to the respective switching field. Figure 2 shows Kerr images[12] of the domain-wall transitions mediat-
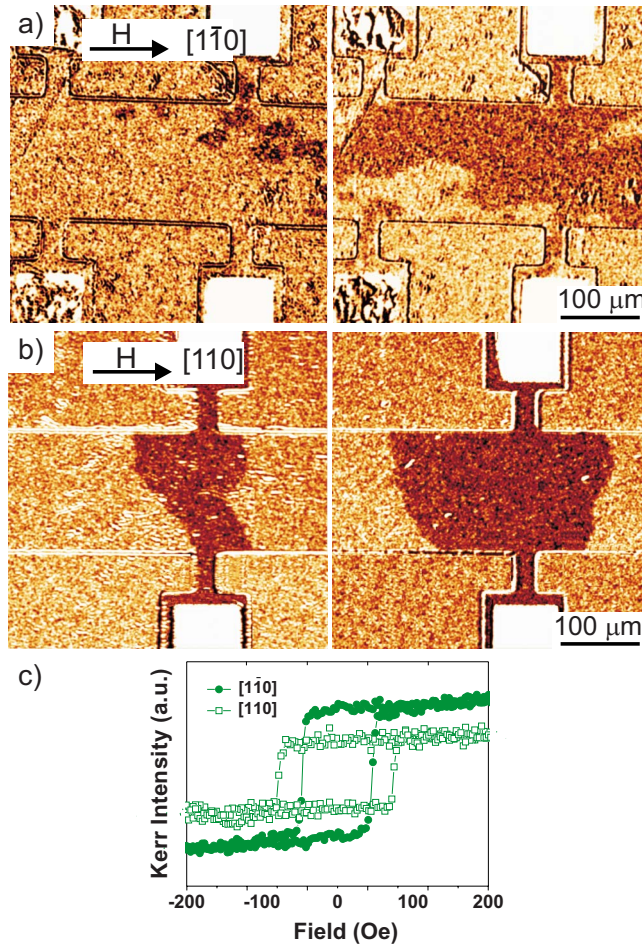

FIG. 2. (Color online) DW nucleation and propagation for the field applied in the [1$\bar{1}$0] (a) and [110] (b) directions at two consecutive times, left and right. The respective hysteresis loops showing single-switching events are displayed in (c). A larger number of domains is found when applying the field along the [1$\bar{1}$0] direction.

ing the magnetization reversal for the field applied along the [1$\bar{1}$0] (a) and [110] (b) directions, respectively. They correspond to hysteresis curves with single switching events displayed in Fig. 2(c). The two Kerr images, left and right in (a) and (b), were taken at consecutive times. A clear asymmetry in the nucleation behavior is observed. For the field applied in the [1$\bar{1}$0] direction [Fig. 2(a)] the reverse domains nucleate in large numbers. In contrast, when the field is applied in the [110] direction (b) the transition is dominated by the propagation of a few DWs nucleated at the contact pads.

In the following we will present evidence supporting the existence of two different kinds of DWs, which seem to be the cause for the asymmetry in the reversal behavior. These two DW types are given by the interplay of the uniaxial and biaxial magnetic anisotropy in compressively strained Ga$_{1-x}$Mn$_x$As epilayers.[13,14] The biaxial component is a spin-orbit coupling effect well described by the theory of hole mediated ferromagnetism. The origin of the uniaxial anisotropy has been related to a small trigonal lattice distortion, but the mechanism leading to this symmetry breaking still remains unclear.[15,16]

Assuming a fourfold crystalline anisotropy plus a uniaxial contribution, the energy of an in-plane single domain state can be described by

$$E = \frac{K_c}{4}\sin^2(2\varphi) + K_u \sin^2(\varphi - 135°) - MH\cos(\varphi - \varphi_H),$$

(1)

where K_c and K_u are the biaxial and uniaxial anisotropy constants, M is the magnetization, H is the magnetic field, and φ and φ_H are the angles of M and H with the [100] direction. The presence of a uniaxial easy axis along the [110] direction shifts the position of the energy minima from the [100] and [010] directions, which are the easy axes in the case of a pure biaxial anisotropy, toward the [110] axis. This shift in angle $\delta/2$ is determined by the ratio between the biaxial and uniaxial anisotropies in the following manner:[8,17]

$$\frac{\delta}{2} = \frac{1}{2}\arcsin\left(\frac{K_u}{K_c}\right).$$

(2)

The value $\delta/2$ can be geometrically derived using the polar plot of the switching fields in the inset of Fig. 3. $\delta/2$ is determined by the angle difference between the corners of the rectangle defined by the first switching fields (green circles) close to the [100] and [010] directions.[18] These corner points are also the directions where first and second switching fields coincide. We obtain $\delta/2$=$(15 \pm 2)°$, indicating that the global easy axes are located $(60 \pm 2)°$ from the [1$\bar{1}$0] direction and $(30 \pm 2)°$ from the [110] direction, respectively.

In order to fit the experimental values of the switching field vs the direction of applied field presented in Fig. 3, the DW nucleation/propagation energy ϵ was equated with the gain in Zeeman energy during the reversal between the initial ($\mathbf{M}_0$) and final ($\mathbf{M}_1$) state of the magnetization in a constant field, ϵ=$\mathbf{H} \cdot (\mathbf{M}_1 - \mathbf{M}_0)$.[19] It has been previously shown[8] that in this case the angle change in the magnetization direction
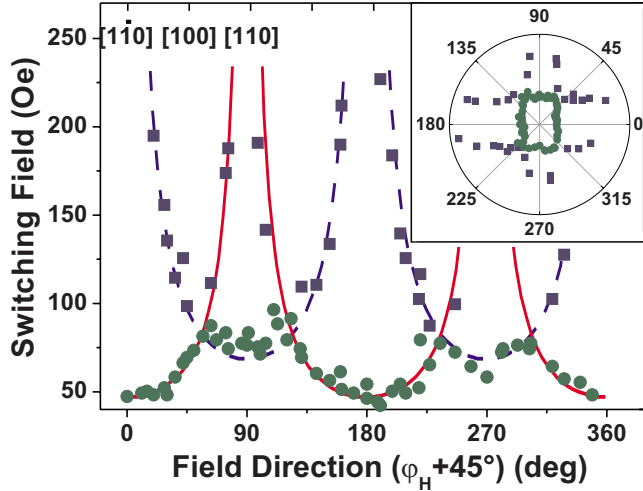
FIG. 3. (Color online) Fits of the experimental results of first- (circles) and second- (squares) switching field vs field angle. The dashed and solid lines represent fits to Eq. (3) considering $90° + \delta$ and $90° − \delta$ DWs, respectively. The value of $\delta/2$ was obtained from the data points as indicated. The data points form two sets of parallel lines when plotted in polar coordinates (inset).

during the reversal can be either $90° + \delta$ or $90° − \delta$, reflecting the shift in the easy axes directions by the angle $\delta/2$. Consequently two expressions accounting for the $90° + \delta$ and $90° − \delta$ transitions have to be considered with corresponding $\epsilon_{90+\delta}$ and $\epsilon_{90-\delta}$. These two expressions for the DW transition $[\epsilon_{90-\delta} = \mathbf{H} \cdot (\mathbf{M}_1 − \mathbf{M}_0)$, $\epsilon_{90+\delta} = \mathbf{H} \cdot (\mathbf{M}'_1 − \mathbf{M}'_0)]$ yield a dependence of the switching field on the angle of the applied field for $90° \pm \delta$ DWs:

$$H_{90\pm\delta} = \frac{\epsilon_{90\pm\delta}}{M\sqrt{2}\cos\left(45 \mp \frac{\delta}{2}\right)[\sin(\varphi_H) \mp \cos(\varphi_H)]}. \quad (3)$$

Using $\delta/2 = (15 \pm 2)°$ and $M = (9.4 \pm 0.1)$ emu/cm^3 we are able to fit the data in Fig. 3 according to Eq. (3) with $\epsilon_{90+\delta}$ and $\epsilon_{90-\delta}$ as fitting parameters. The two functions shown in Fig. 3 reproduce very well the two branches of the switching field observed in the MOKE measurement. The solid line represents the $90° − \delta$ (60° DW) transition with the corresponding value for the nucleation/propagation energy of $\epsilon_{90-\delta} = 460$ J/cm^3. The dashed line models the $90° + \delta$ (120° DW) reversal process with $\epsilon_{90+\delta} = 1173$ J/cm^3. Taking this into account, the switching field obtained with the field oriented along the $[1\bar{1}0]$ direction would correspond to a 60° DW since the experimental value for the switching field lays on the solid fit curve. Similarly, for the field applied in the [110] axis, the switching field is found on the dashed fit curve and consequently corresponds to a 120° DW. As discussed earlier these two types of DWs seem to show a very different nucleation/propagation behavior.

According to Fig. 3 the second transition cannot be triggered within the available magnetic-field range when the fields are applied either along the $[1\bar{1}0]$ or the [110] directions. However, to corroborate the observations for the field applied along these two directions, the nucleation has been studied for fields applied in the [100] direction. In this case
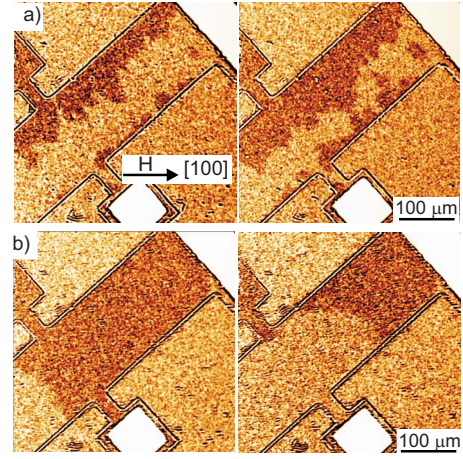
the longitudinal axis of the Hall bar was fixed at an angle of 45° with respect to the direction of the field. According to the plot of switching field vs field angle in Fig. 3, in the [100] direction ($\varphi_H = 0°$) both of the two transitions can be observed, which add up to a full 180° reorientation. The two switching events are clearly visible in the MOKE signal in Fig. 1(a). According to the fit in Fig. 3, the first switching field along the [100] axis corresponds to a 60° DW transition and the second to a 120° DW. In analogy with the previously shown dynamics a larger number of nucleation centers are expected for the first switching field (lying on the solid line of the fitting curve) and only few domains for the second switching field (lying on the dashed line of the fitting curve), suggesting a DW-propagation-dominated reversal. The results shown in Figs. 4(a) and 4(b) (first and second transition, respectively) confirm this prognosis and therefore support the notion of the presence of two species of DWs with different dynamics. Figure 4(a) corresponds to the first jump in the Kerr signal found after saturation as indicated with filled symbols in Fig. 1(a). Figure 4(b) shows the subsequent single domain-wall transition indicated by the open symbols, respectively.

From the fitting we extracted a ratio of ϵ for the two types of DWs of $(\epsilon_{90+\delta}/\epsilon_{90-\delta}) = 2.5$. The experimental results thus indicate a considerably lower nucleation/propagation energy for the $90° − \delta$ transition with respect to $90° + \delta$. At the same time KM proves that low ϵ values are correlated with a larger number of nucleation sites. We therefore conclude that the dynamics shifts from a propagation-dominated regime to a partly nucleation-dominated one for high and low ϵ, respectively. In the former case the observed low number of domains is most likely determined by a few isolated defects within the Hall devices serving as nucleation centers.

Finally, we shortly want to discuss the special quantity ϵ/M given by the value of the switching field at exactly the crossing point of the fitting lines ($\varphi_H = 15°$), where only one switching event occurs. As discussed earlier, this point defines the global easy axes direction of the system. The quan-

FIG. 4. (Color online) Kerr images of DWs involved in the (a) first- and (b) second-switching event for the field applied along the [100] direction at two consecutive times, left and right. In the MOKE hysteresis loop an intermediate plateau appears between the first- and the second-switching event [see Fig. 1(a)].

tity ϵ/M is of interest for a comparison of the material used here with materials grown in other laboratories. Gould *et al.*[19] give a list of values with ϵ/M ranging between 7.1 and 18 mT for $Ga_{1-x}Mn_xAs$ materials grown in various well-known MBE facilities. Our value $\epsilon/M = 8.7$ mT falls well into that range, confirming the comparability of our material to other high-quality materials in the literature.

In conclusion, extensive MOKE and Kerr-microscopy studies of the nucleation of domains and the propagation behavior of DWs in $Ga_{1-x}Mn_xAs$ Hall bar devices revealed substantially different dynamics for two observed species of DWs. They correspond to $90° \pm \delta$ DWs, and they originate from the uniaxial part of the magnetic anisotropy. While the $90° + \delta$ reversal is found to be propagation dominated with a small number of domains, the $90° - \delta$ case involves a larger number of nucleation centers. The measured coercivities for both reversals can be very well fitted by a model which includes the uniaxial anisotropy contribution. From the fits a considerably lower nucleation/propagation energy ϵ for the $90° - \delta$ transition with respect to the $90° + \delta$ transition is derived, which suggests an inverse correlation of ϵ with the number of nucleated domains. In the case of $90° + \delta$ the observed low number of domains is determined by few defects within the Hall devices serving as nucleation centers, which opens the possibility to design single domain devices, e.g., for magnetologic elements.

---

*Present address: Department of Physics and Astronomy, University of Nebraska, Lincoln, NE 68588, USA.

†Present address: Department of Physics, University of Fribourg, Chemin du Musée 3, CH-1700 Fribourg, Switzerland.

‡Present address: Forschungszentrum Karlsruhe, Institut für Festkörperphysik, 76021 Karlsruhe, Germany.

§j.honolka@fkf.mpg.de

[1] H. Ohno, Science **281**, 951 (1998).

[2] T. Dietl, H. Ohno, F. Matsukura, J. Cibert, and D. Ferrand, Science **287**, 1019 (2000).

[3] D. Chiba, F. Matsukura, and H. Ohno, Appl. Phys. Lett. **89**, 162505 (2006).

[4] D. A. Allwood, G. Xiong, C. C. Faulkner, D. Atkinson, D. Petit, and R. P. Cowburn, Science **309**, 1688 (2005).

[5] A. Hubert and R. Schaefer, *Magnetic Domains* (Springer-Verlag, Berlin, 1998).

[6] Sug-Bong Choe and S.-C. Shin, IEEE Trans. Magn. **36**, 3167 (2000).

[7] M. Yamanouchi, D. Chiba, F. Matsukura, and H. Ohno, Nature (London) **428**, 539 (2004).

[8] K. Pappert, C. Gould, M. Sawicki, J. Wenisch, K. Brunner, G. Schmidt, and L. W. Molenkamp, New J. Phys. **9**, 354 (2007).

[9] H. X. Tang, R. K. Kawakami, D. D. Awschalom, and M. L. Roukes, Phys. Rev. Lett. **90**, 107201 (2003).

[10] U. Welp, V. K. Vlasko-Vlasov, X. Liu, J. K. Furdyna, and T. Wojtowicz, Phys. Rev. Lett. **90**, 167206 (2003).

[11] J. Sadowski, J. Z. Domagala, J. Bak-Misiuk, S. Koleśnik, M. Sawicki, K. Świątek, J. Kanski, L. Ilver, and V. Strom, J. Vac. Sci. Technol. B **18**, 1697 (2000).

[12] I. Horcas, R. Fernández, J. M. Gómez-Rodríguez, and J. Colchero, Rev. Sci. Instrum. **78**, 013705 (2007).

[13] D. Hrabovsky, E. Vanelle, A. R. Fert, D. S. Yee, J. P. Redoules, J. Sadowski, J. Kanski, and L. Ilver, Appl. Phys. Lett. **81**, 2806 (2002).

[14] K. Y. Wang, M. Sawicki, K. W. Edmonds, R. P. Campion, S. Maat, C. T. Foxon, B. L. Gallagher, and T. Dietl, Phys. Rev. Lett. **95**, 217204 (2005).

[15] T. Jungwirth, J. Sinova, J. Mašek, J. Kučera, and A. H. MacDonald, Rev. Mod. Phys. **78**, 809 (2006).

[16] M. Sawicki, K.-Y. Wang, K. W. Edmonds, R. P. Campion, C. R. Staddon, N. R. S. Farley, C. T. Foxon, E. Papis, E. Kaminska, A. Piotrowska, T. Dietl, and B. L. Gallagher, Phys. Rev. B **71**, 121302(R) (2005).

[17] C. Daboo, R. J. Hicken, D. E. P. Eley, M. Gester, S. J. Gray, A. J. R. Ives, and J. A. C. Bland, J. Appl. Phys. **75**, 5586 (1994).

[18] C. Gould, S. Mark, K. Pappert, R. G. Dengel, J. Wenisch, R. P. Campion, A. W. Rushforth, D. Chiba, Z. Li, X. Liu, W. Van Roy, H. Ohno, J. K. Furdyna, B. Gallagher, K. Brunner, G. Schmidt, and L. W. Molenkamp, New J. Phys. **10**, 055007 (2008).

[19] R. P. Cowburn, S. Gray, J. Ferré, J. Bland, and J. Miltat, J. Appl. Phys. **78**, 7210 (1995).